NANO LETTERS

2009
Vol. 9, No. 5
2094-2098

Indirect Excitons in Elevated Traps

A. A. High,*,† A. T. Hammack,† L. V. Butov,† L. Mouchliadis,‡ A. L. Ivanov,‡ M. Hanson,§ and A. C. Gossard§

Department of Physics, University of California at San Diego, La Jolla, California 92093-0319, Department of Physics and Astronomy, Cardiff University, Cardiff CF24 3AA, United Kingdom, and Materials Department, University of California at Santa Barbara, Santa Barbara, California 93106-5050

Received February 25, 2009; Revised Manuscript Received April 10, 2009

ABSTRACT

We report on the study of indirect excitons in elevated traps. The transition from a normal to elevated trap results in the appearance of narrow lines in the emission spectrum. The density, temperature, and voltage dependences indicate that these lines correspond to the emission of individual states of indirect excitons in a disorder potential in the elevated trap.

An indirect exciton in a coupled quantum well (CQW) structure is composed of an electron and a hole in separated QWs (Figure 1a). Indirect excitons in a CQW have a dipole moment ed, where d is close to the distance between the QW centers, and their energy can be controlled by the transverse electric field F_z, which shifts the exciton energy by edF_z[1] (Figure 1b). This allows creation of in-plane potential profiles for the indirect excitons $E(x,y) = edF_z(x,y) \propto V(x,y)$ by a laterally modulated gate voltage $V(x,y)$. Indirect excitons were studied in various electrostatically created potential profiles including ramps,[2,3] lattices,[4−7] traps,[6,8,9] and circuit devices.[10,11]

In this paper, we report on the study of indirect excitons in a new trap—the elevated trap. In-plane potential profiles were created by the pattern of electrodes shown in Figure 1c. Elevated traps for indirect excitons in the region of central electrode t were created by applying $|V_t| < |V_g|,|V_s|$, while normal traps were created by applying $|V_t| > |V_g|,|V_s|$. The energy of the elevated trap is above the energy of its surroundings, $E_t > E_g,E_s$ (Figure 2a), while the energy of the normal trap is below, $E_t < E_g,E_s$ (Figure 2c).

The CQW structure was grown by MBE. An n^+-GaAs layer with $n_{Si} = 10^{18}$ cm^{-3} serves as a homogeneous bottom electrode. The top electrodes on the surface of the structure were fabricated by depositing a semitransparent layer of Pt (8 nm) and Au (2 nm). Two 8 nm GaAs QWs separated by a 4 nm $Al_{0.33}Ga_{0.67}As$ barrier were positioned 0.1 μm above the n^+-GaAs layer within an undoped 1 μm thick $Al_{0.33}Ga_{0.67}As$ layer. Positioning the CQW closer to the homogeneous electrode suppresses the in-plane electric field,[6]

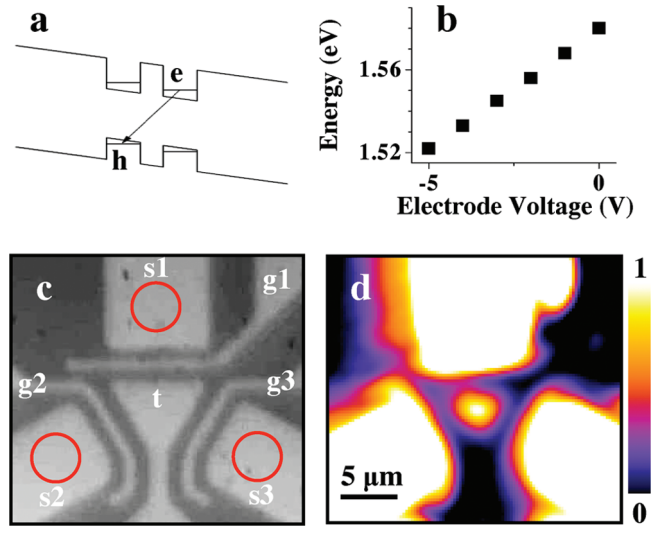

Figure 1. (a) Energy band diagram of the CQW structure: e, electron; h, hole. (b) Energy of indirect excitons vs electrode voltage (applies for all electrodes on the sample). (c) Electrode pattern. A trap is formed at electrode t by voltages on electrodes s, g, and t. The circles show the positions of the laser excitation. (d) Emission image of indirect excitons in the elevated trap regime. The cloud of indirect excitons in the elevated trap is in the center. $V_s = -2$ V, $V_g = -1.5$ V, $V_t = -0.5$ V, $P_{ex} = 750$ μW, $T = 1.4$ K.

which otherwise can lead to exciton dissociation.[4] The excitons were photoexcited by a 633 nm HeNe laser focused to a spot ~5 μm in diameter in the area shown by the upper circle in Figure 1c (except for the data in Figure 1d, which was measured with three excitation spots at the three circles in Figure 1c, the results with one and three excitation spots were qualitatively similar). For the elevated trap regime, excitons in the trap were mainly created by the tail of the laser excitation which reduced heating in the trap area. The emission images were taken by a CCD with an interference

* Corresponding author, alex.high@gmail.com.
† Department of Physics, University of California at San Diego.
‡ Department of Physics and Astronomy, Cardiff University.
§ Materials Department, University of California at Santa Barbara.

10.1021/nl900605b CCC: $40.75
Published on Web 04/21/2009

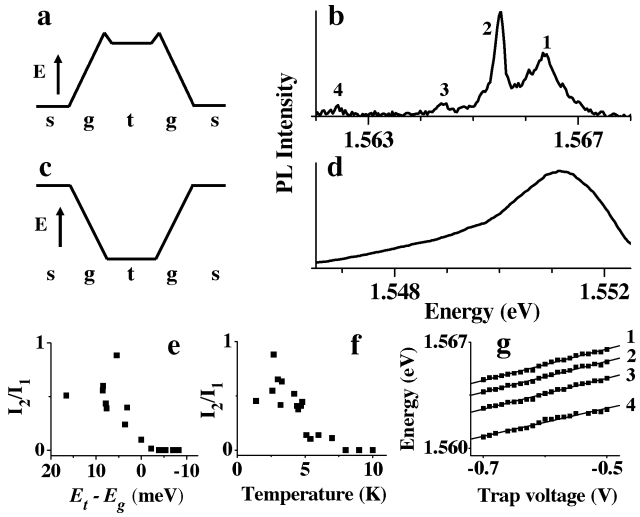

Figure 2. (a) Schematic of an elevated trap. (b) Emission spectra of indirect excitons in the elevated trap. $V_s = -2$ V, $V_g = -1.5$ V, $V_t = -0.5$ V. (c) Schematic of a normal trap. (d) Emission spectra of indirect excitons in the normal trap. $V_s = -2$ V, $V_g = -2.5$ V, $V_t = -3.5$ V. (e) The ratio of line 2 to line 1 intensities I_2/I_1 vs energy difference between the indirect excitons in the trap and surrounding gates. (f) I_2/I_1 vs bath temperature. $V_s = -2$ V, $V_g = -1.5$ V, $V_t = -0.5$ V, $P_{ex} = 6.3$ μW. (g) Energies of lines 1−4 vs V_t. $V_s = -2$ V, $V_g = -1.5$ V. For (b, d, e, g), $T = 1.4$ K and $P_{ex} = 18$ μW.

filter 800 ± 5 nm, which covers the spectral range of the indirect excitons. The spatial resolution was 1.5 μm. The spectra were measured using a spectrometer with resolution 0.18 meV. All presented spectra were taken from the trap center.

For the entire range of studied densities ($P_{ex} = 1-1140$ μW with the smallest limited by signal strength) the emission spectrum in the normal trap was a structureless line with full width at half-maximum (fwhm) >1 meV, like that in Figure 2d. However, sharp lines were observed in the emission spectrum in the elevated trap (Figure 2b). fwhm of lines 2−4 were measured as low as 0.18 meV, which is close to the spectrometer resolution. The sharp lines vanish at the transition from the elevated trap to normal trap, i.e., at $E_t \approx E_g$ (Figure 2e). They also vanish with increasing bath temperature (Figure 2f).

Varying the electrode voltage V_t results in an energy shift of lines 1−4, Figure 2g. The measured $\delta E \approx 10.4 V_t$ meV/V corresponds to $d \approx 10.7$ nm, which is close to the nominal distance between the QW centers. Therefore, lines 1−4 correspond to the emission of indirect excitons. Note that sharp lines in the emission of excitons in QWs were observed earlier.[12−14] They were attributed to the emission of excitons localized in local minima of the in-plane disorder potential. The latter forms mainly due to QW width and alloy fluctuations.[12−17] In contrast to the sharp lines in Figure 2, the sharp lines in refs 12−14 correspond to the emission of *direct* excitons with both electrons and holes confined in one QW.

In analogy to the interpretation of sharp lines corresponding to the emission of direct excitons,[12−14] we attribute the observed sharp lines (Figure 2b) to the emission of indirect excitons localized in local minima of the disorder potential in the trap. We note that the local minima of a disorder potential can be considered as "natural quantum dots";[12] in turn, natural quantum dots for indirect excitons can be considered as a counterpart of quantum dot pairs and posts.[18−21]

In general, the particle localization length is small for the lowest energy states in a disorder potential and increases with increasing energy.[22] The particle can be considered as localized when the localization length is small compared to the system size, the trap size in our case, and delocalized (over the system) when the localization length is comparable to the system size. The density dependence presented below indicates that low-energy lines 2−4 correspond to the emission of localized states, while high-energy line 1 (which can be a set of unresolved narrower lines) corresponds to the emission of delocalized excitons.

First, we discuss why the sharp lines are observed in the elevated trap regime and vanish in the normal trap regime. The observation of individual localized states in the disorder potential is facilitated by collecting the exciton emission from a small area (Figure 1d) containing not too many localized states so that their emission can be resolved. However, both the normal and elevated traps utilize the small area, while sharp lines emerge only in the elevated trap regime (Figure 2e). Their emergence is facilitated by an effective "cooling" of the excitons present only in an elevated trap. Since the energy of excitons in the elevated trap is higher than that in the surrounding areas, excitons can escape the trap. The escape rate of lower-energy strongly localized excitons is generally slower. This increases the occupation of lower-energy strongly localized states in comparison to that of higher-energy weakly localized (or delocalized) states. An increase in the relative occupation of lower-energy states can be considered as lowering the exciton temperature. This mechanism has similarities with evaporative cooling. In turn, the sharp lines vanish with increasing temperature (Figure 2f) and in the normal trap regime where "evaporative cooling" is absent (Figure 2e).[23]

One can introduce an effective temperature $\tilde{T}$ for the population balance between the localized and delocalized states as $\delta = n_{deloc}/n_{loc} \sim \exp[-\varepsilon/(k_B\tilde{T})]$, where ε is a localization energy. Then the "cooling efficiency" in the elevated trap regime can be quantified by the parameter $\gamma = \delta_{norm}/\delta_{elev}$. A large γ observed in the experiments indicates an efficient cooling. In turn, the temperatures in the elevated trap regime and in the normal trap regime are related by $1/\tilde{T}_{elev} = 1/\tilde{T}_{norm} + (k_B/\varepsilon) \ln \gamma$. This allows a rough estimate for $\tilde{T}_{elev}$. Assuming $\gamma \gtrsim 10$ and $\varepsilon/k_B \sim 10$ K (corresponding to line 2, Figure 2) and $\tilde{T}_{norm} \sim 3$ K (corresponding to a typical temperature of the indirect excitons in the presence of continuous wave excitation and without the "cooling"),[24,25] one obtains $\tilde{T}_{elev} \lesssim 1.8$ K.

The "cooling efficiency" γ can be estimated by using the rate equations for occupations of the localized and delocalized states at equilibrium, which result to $\gamma = 1 + \tau/\tau_{esc}$, where $\tau^{-1} = \Lambda^{-1}\tau_{loc}^{-1} + \tau_{opt}^{-1}$, $\Lambda^{-1} = (\Lambda_l + \Lambda_d)/\Lambda_l$, Λ_d (Λ_l) is the population rate of the delocalized (localized) states

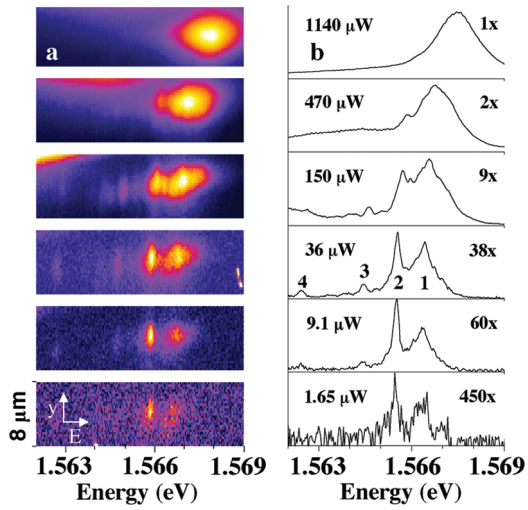

Figure 3. (a) $E-y$ emission images and (b) spectra of indirect excitons in the elevated trap vs P_{ex}. $V_s = -2$ V, $V_g = -1.5$ V, $V_t = -0.5$ V, $T = 1.4$ K. P_{ex} values and magnifications are indicated on (b).

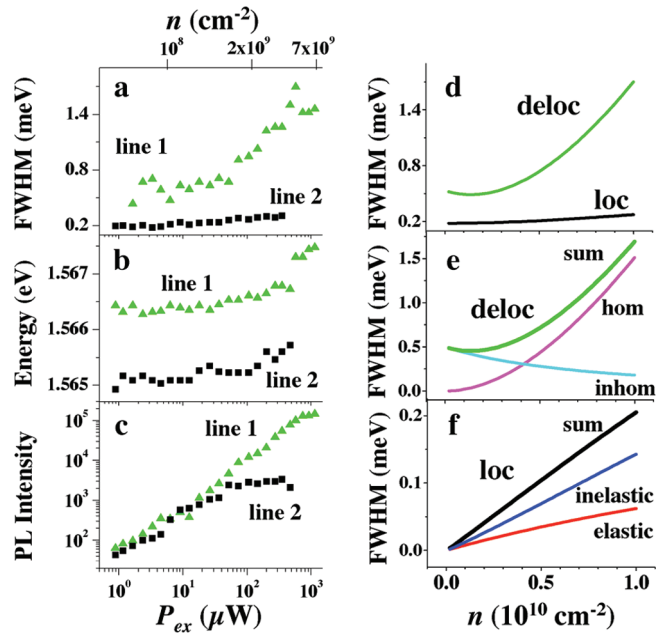

Figure 4. (a) fwhm, (b) energy, and (c) intensity of line 1 (green triangles) and line 2 (black squares) vs P_{ex}. Density listed on top is an estimate based on the exciton energy shift; the lowest value is an estimate based on the PL intensity ratio. $V_s = -2$ V, $V_g = -1.5$ V, $V_t = -0.5$ V, $T = 1.4$ K. (e) Calculated fwhm of emission line of delocalized indirect excitons (green). Thin lines present the contributions from homogeneous broadening due to exciton−exciton interaction (magenta) and inhomogeneous broadening due to disorder (cyan). The disorder amplitude $U^{(0)}/2 = 0.35$ meV corresponds to line 1. (f) Calculated fwhm of emission line of localized indirect excitons (black). Thin lines present the contributions from inelastic (blue) and elastic (red) exciton scattering. $\varepsilon = 1.3$ meV corresponds to line 2. (d) Calculated fwhm of emission lines including the resolution 0.18 meV for comparison with the experimental data in (a).

due to the laser excitation, τ_{opt} and τ_{loc} are the radiative and localization times of the delocalized excitons, and τ_{esc} is their escape time from the elevated trap ($\tau_{esc} \sim S_{trap}/D_x \sim 0.1-1$ ns for elevated trap area $S_{trap} \sim 1$ μm^2 and diffusion coefficient $D_x \sim 10-100$ cm^2/s [26]). For direct excitons with a short lifetime $\tau_{opt} \sim 0.01-0.1$ ns, the cooling is inefficient. Indeed, in this case $\gamma < 1 + \tau_{opt}/\tau_{esc} \sim 1.1$. On the contrary, the cooling can be efficient for indirect excitons with a long lifetime $\tau_{opt} \sim 10-10^4$ ns. In this case $\gamma \sim 1 + \Lambda\tau_{loc}/\tau_{esc}$. It reaches $\gamma \sim 10$ estimated from the experiments when $\tau_{esc} \sim 0.1\Lambda\tau_{loc}$.

The density dependence of the emission of indirect excitons in the elevated trap is presented in Figures 3 and 4. In the entire studied density range, states 1−4 are confined in the elevated trap. This confinement is revealed by the finite spatial extension of all states in the trap ~3 μm (Figures 1d and 3a). (Note parenthetically that the confinement may involve a small barrier at the trap edges, shown schematically in Figure 2a; however the exact trap profile is beyond the scope of this paper.) The features of the density dependence are considered below.

The exciton energy increases with density due to the repulsive dipole−dipole interaction of the indirect excitons (Figures 3 and 4b). The exciton density n can be estimated from the energy shift δE as $n = \varepsilon\delta E/(4\pi e^2 d)$.[27−30] It is presented at the top of parts a−c of Figure 4. The energy shift of the localized states is close to that of the delocalized states.

The emission intensity of the localized excitons saturates as shown in Figure 4c for line 2. The saturation indicates that only a finite a number of excitons can occupy a local minimum of the disorder potential. For the minimum corresponding to line 2, this number appears to be 1. Indeed, if a second exciton were added to the minimum, the energy of the exciton state in it would increase due to the repulsive interaction. Since the area of the minimum is small compared to the area of the entire trap, adding one more exciton should result in a significant increase of the exciton density in it and, in turn, a sharp increase of the energy of the localized state. Since no such energy increase is observed (Figure 4b), no more than 1 exciton can occupy the local potential minimum. This is consistent with the small estimated exciton localization length in the minimum $l_{loc} \sim \hbar/(2M_x\varepsilon)^{1/2} \sim 10$ nm, comparable to the exciton Bohr radius. The effect is similar to the Coulomb blockade for electrons. It is due to the dipole−dipole repulsion of the indirect excitons.

The emission lines broaden with density (Figures 3b and 4a). While the widths of lines 2−4 increase by only about 0.1 meV, the width of line 1 increases by more than 1 meV (Figure 4a). The strong difference indicates that lines 2−4 correspond to the emission of localized states, while line 1 is delocalized, as discussed below.

The spectral width of the delocalized state emission is approximated by $\Delta_{fwhm} = [\Gamma_{hom}^2 + \Gamma_{inhom}^2]^{1/2}$, where $\Gamma_{hom} = \hbar/\tau_{x-x} + \hbar/\tau_{x-LA} + \hbar/\tau_{rec}$ is the homogeneous broadening due to exciton−exciton and exciton−phonon scattering and finite recombination lifetime and $\Gamma_{inhom} = \langle U_{rand}\rangle$ is the inhomogeneous broadening due to disorder, $\langle U_{rand}\rangle$ is the average amplitude of the CQW in-plane long-range disorder potential. For $n \gtrsim 10^8$ cm^{-2} relevant to the experiments, Γ_{hom} is well approximated by $\hbar/\tau_{x-x}$ with τ_{x-x} given by

$$\frac{1}{\tau_{x\text{-}x}} = \left(\frac{u_0 M_x}{2\pi}\right)^2 \left(\frac{k_B T}{\hbar^5}\right) e^{-T_0/T} F_0 \int_0^\infty du \int_0^{2\pi} d\phi \times \frac{e^{2u}}{[e^{u(1-\cos\phi)} - F_0][e^{u(1+\cos\phi)} - F_0][e^{2u} - F_0]} \quad (1)$$

where $F_0 = 1 - e^{-T_0/T}$, $T_0 = \pi\hbar^2 n/(2M_x)$, and u_0 is approximated by $u_0 \simeq 4\pi e^2 d/\epsilon$.[31] In this sample, excitons have mass $M_x = 0.22 m_0$. $\Gamma_{hom}(n)$ evaluated with eq 1 is shown in Figure 4e.

The inhomogeneous broadening is dominant at low densities where the interaction effects vanish. It produces a line width of 0.5 meV for the studied sample, Figure 4a. The inhomogeneous broadening decreases with increasing density due to screening of the long-range disorder potential by interacting indirect excitons as

$$\Gamma_{inhom} = \frac{U^{(0)}}{1 + [(2M_x)/(\pi\hbar^2)](e^{T_0/T} - 1)u_0} \quad (2)$$

where $U^{(0)} = 2\langle |U_{rand}(\mathbf{r}_{||})| \rangle$ is the amplitude of the unscreened disorder potential, when $n \rightarrow 0$.[30] $\Gamma_{inhom}(n)$ evaluated with eq 2 is shown in Figure 4e.

The density increase also results in the homogeneous broadening of the localized states, lines 2−4 (Figure 4a), due to the scattering of the localized exciton with delocalized excitons. It is given by $\Gamma_{hom}^{(loc)} = \hbar/\tau_{in} + \hbar/\tau_{el}$ with

$$\frac{\hbar}{\tau_{in}} = \left(\frac{u_0 M_x}{2\pi\hbar^2}\right)^2 k_B T(1 + F_0) F_0 \int_{2\Delta}^\infty du \int_0^{2\pi} d\phi \times \frac{e^{2u}}{[e^{u-\Delta-f(u)\cos\phi} - F_0][e^{u-\Delta+f(u)\cos\phi} - F_0][e^{2u} - F_0]} \quad (3)$$

$$\frac{\hbar}{\tau_{el}} = \left(\frac{u_0 M_x}{2\pi\hbar^2}\right)^2 k_B T F_0 \int_0^\infty du \int_0^{2\pi} d\phi \frac{e^{u/\cos 2\phi}}{[e^{u/\cos 2\phi} - F_0][e^{u\tan 2\phi} - F_0]} \quad (4)$$

where $f(u) = (u(u - 2\Delta))^{1/2}$ and $\Delta = \varepsilon/(2k_B T)$. The first (second) contribution is due to the inelastic (elastic) scattering channel "localized exciton + delocalized exciton → delocalized (localized) exciton + delocalized exciton". In elastic scattering the delocalized exciton changes its momentum by the amount which can be relaxed by the localized exciton, $\sim 1/l_{loc}$. The numerical evaluations with eqs 1, 3, and 4 show that the homogeneous broadening of the localized state is much smaller than that of the delocalized state (Figure 4e,f). This difference can be attributed to the energy gap ε, which reduces the number of possible states for the scattering of localized excitons. This difference in line width broadening with increasing density allows distinguishing the localized from delocalized states and attribute lines 2−4 to the former and lines 1 to the latter. The theoretical and experimental results are in agreement; compare parts a and d of Figure 4.

Acknowledgment. This work is supported by ARO, DOE, NSF, and WIMCS.

Supporting Information Available: Additional information on the experimental conditions required to observe the emission or individual states of indirect excitons localized in local minima of the disorder potential. This material is available free of charge via the Internet at http://pubs.acs.org.

References

(1) Miller, D. A. B.; Chemla, D. S.; Damen, T. C.; Gossard, A. C.; Wiegmann, W.; Wood, T. H.; Burrus, C. A. Electric Field Dependence of Optical Absorption Near the Bandgap of Quantum Well Structures. *Phys. Rev. B: Condens. Matter Mater. Phys.* **1985**, *32*, 1043–1060.

(2) Hagn, M.; Zrenner, A.; Böhm, G.; Weimann, G. Electric-Field-Induced Exciton Transport in Coupled Quantum Well Structures. *Appl. Phys. Lett.* **1995**, *67*, 232.

(3) Gartner, A.; Holleithner, A. W.; Kotthaus, J. P.; Schul, D. Drift Mobilitiy of Long-Living Excitons in Coupled GaAs Quantum Wells. *Appl. Phys. Lett.* **2006**, *89*, 052108.

(4) Zimmermann, S.; Govorov, A. O.; Hansen, W.; Kotthaus, J. P.; Bichler, M.; Wegscheider, W. Lateral Superlattices as Voltage-Controlled Traps for Excitons. *Phys. Rev. B* **1997**, *56*, 13414.

(5) Krau*β*, J.; Kotthaus, J. P.; Wixforth, A.; Hanson, M.; Driscoll, D. C.; Gossard, A. C.; Schuh, D.; Bichler, M. Capture and Release of Photonic Images in a Quantum Well. *Appl. Phys. Lett.* **2004**, *85*, 5830.

(6) Hammack, A. T.; Gippius, N. A.; Yang, Sen; Andreev, G. O.; Butov, L. V.; Hanson, M.; Gossard, A. C. Excitons in Electrostatic Traps. *J. Appl. Phys.* **2006**, *99*, 066104.

(7) Remeika, M.; Graves, J. C.; Hammack, A. T.; Meyertholen, A. D.; Fogler, M. M.; Butov, L. V. Localization-Delocalization Transition of Indirect Excitons in Lateral Electrostatic Lattices, arXiv:0901.1349, 2009.

(8) Huber, T.; Zrenner, A.; Wegscheider, W.; Bichler, M. Electrostatic Exciton Traps. *Phys. Status Solidi A* **1998**, *166*, R5.

(9) Chen, G.; Rapaport, R.; Pffeifer, L. N.; West, K.; Platzman, P. M.; Simon, S.; Vörös, Z.; Snoke, D. Artificial Trapping of a Stable High-Density Dipolar Exciton Fluid. *Phys. Rev. B* **2006**, *74*, 045309.

(10) High, A. A.; Hammack, A. T.; Butov, L. V.; Hanson, M.; Gossard, A. C. Exciton Optoelectronic Transistor. *Opt. Lett.* **2007**, *32*, 2466.

(11) High, A. A.; Novitskaya, E. E.; Butov, L. V.; Hanson, M.; Gossard, A. C. Control of Exciton Fluxes in an Excitonics Integrated Circuit. *Science* **2008**, *321*, 229.

(12) Zrenner, Z.; Butov, L. V.; Hagn, M.; Abstreiter, G.; Böhm, G.; Weimann, G. Quantum Dots Formed by Interface Fluctuations in AlAs/GaAs Coupled Quantum Well Structures. *Phys. Rev. Lett.* **1994**, *72*, 3382.

(13) Hess, H. F.; Betzig, E.; Harris, T. D.; Pfeiffer, L. N.; West, K. W. Near-Field Spectroscopy of the Quantum Constituents of a Luminescent System. *Science* **1994**, *264*, 1740.

(14) Gammon, D.; Snow, E. S.; Shanabrook, B. V.; Katzer, D. S.; Park, D. Fine Structure Splitting in the Optical Spectra of Single GaAs Quantum Dots. *Phys. Rev. Lett.* **1996**, *76*, 3005.

(15) Hegarty, J.; Goldner, L.; Sturge, M. D. Localized and Delo-calized 2D Excitons in GaAs-Al_xGa_{1-x}As Multiple Quantum Well Structures. *Phys. Rev. B* **1984**, *30*, 7346.

(16) Takagahara, T. Localization and Energy Transfer of Quasi-Two-Dimensional Excitons in GaAs-AlAs Quantum-Well Heterostructures. *Phys. Rev. B* **1985**, *31*, 6552.

(17) Zimmermann, Z.; Runge, E. Excitons in Narrow Quantum Wells: Disorder Localization and Luminescence Kinetics. *Phys. Status Solidi A* **1997**, *164*.

(18) Krenner, H. J.; Sabathil, M.; Clark, E. C.; Kress, A.; Schuh, D.; Abstreiter, G.; Finley, J. J. Direct Observation of Controlled Coupling in an Individual Quantum Dot Molecule. *Phys. Rev. Lett.* **2005**, *94*, 057402.

(19) Stinaff, A. E.; Scheibner, M.; Bracker, A. S.; Ponomarev, I. V.; Korenev, V. L.; Ware, M. E.; Doty, M. F.; Reinecke, T. L.; Gammon, D. Optical Signatures of Coupled Quantum Dots. *Science* **2006**, *636*, 3869.

(20) Scheibner, M.; Ponomarev, I. V.; Stinaff, A. E.; Doty, M. F.; Bracker, A. S.; Hellberg, C. S.; Reinecke, T. L.; Gammon, D. Photoluminescence Spectroscopy of the Molecular Biexciton in Vertically Stacked InAs-GaAs Quantum Dot Pairs. *Phys. Rev. Lett.* **2007**, *99*, 197402.

(21) Krenner, H. J.; Pryor, C. E.; Jun, He; Petroff, P. M. A. Semiconductor Exciton Memory Cell Based on a Single Quantum Nanostructure. *Nano Lett.* **2008**, *8*, 1750.

(22) Lee, P. A.; Ramakrishnan, T. V. Disordered Electronic Systems. *Rev. Mod. Phys.* **1985**, *57*, 287.

(23) Note that in the normal trap the excitons travel to the trap center downhill potential energy gradient that may increase the exciton temperature.[24] In turn, in the elevated trap traveling uphill may reduce the exciton temperature. However, in the presented experiments this

is inessential since the estimated number of excitons which can overpass the potential energy hill and reach the elevated trap is small compared to the number of excitons created in the trap due to the tails of the laser excitation.
(24) Hammack, A. T.; Griswold, M.; Butov, L. V.; Smallwood, L. E.; Ivanov, A. L.; Gossard, A. C. Trapping of Cold Excitons in Quantum Well Structures with Laser Light. *Phys. Rev. Lett.* **2006**, *26*, 227402.
(25) Butov, L. V.; Ivanov, A. L.; Imamoglu, A.; Littlewood, P. B.; Shashkin, A. A.; Dolgopolov, V. T.; Campman, K. L.; Gossard, A. C. Stimulated Scattering of Indirect Excitons in Coupled Quantum Wells: Signature of a Degenerate Bose-Gas of Excitons. *Phys. Rev. Lett.* **2001**, *86*, 5608.
(26) Ivanov, A. L.; Smallwood, L. E.; Hammack, A. T.; Yang, Sen; Butov, L. V.; Gossard, A. C. Origin of the Inner Ring in Photoluminescence Patterns of Quantum Well Excitons. *Europhys. Lett.* **2006**, *73*, 920.
(27) Yoshioka, D.; MacDonald, A. H. Double Quantum Well Electron-Hole Systems in Strong Magnetic Fields. *J. Phys. Soc. Jpn.* **1990**, *59*, 4211.
(28) Zhu, X.; Littlewood, P. B.; Hybertsen, M.; Rice, T. Exciton Condensate in Semiconductor Quantum Well Structures. *Phys. Rev. Lett.* **1995**, *74*, 1633.
(29) Lozovik, Yu. E.; Berman, O. L. Phase Transitions in a System of Two Coupled Quantum Wells. *JETP Lett.* **1996**, *64*, 573.
(30) Ivanov, A. L. Quantum Diffusion of Dipole-Oriented Indirect Excitons in Coupled Quantum Wells. *Europhys. Lett.* **2002**, *59*, 586.
(31) Ivanov, A. L.; Haug, H.; Littlewood, P. B. Bose-Einstein Statistics in Thermalization and Photoluminescence of Quantum-Well Excitons. *Phys. Rev. B* **1999**, *59*, 5032.

NL900605B